Available online at www.sciencedirect.com
ScienceDirect
Spectrochimica Acta Part A 68 (2007) 211–219
SPECTROCHIMICA ACTA PART A
www.elsevier.com/locate/saa

# Synthesis, thermal and spectral studies of first-row transition metal complexes with girard P reagent-based ligand

Usama El-Ayaan *, I.M. Kenawy, Y.G. Abu El-Reash

*Department of Chemistry, Faculty of Science, Mansoura University, Mansoura 35516, Egypt*

Received 7 October 2006; received in revised form 9 November 2006; accepted 17 November 2006

**Abstract**

A new series of first-row transition metal complexes with 1-acetylpyridinium chloride-4-benzoyl thiosemicarbazide ($H_2$GPBzIT) have been prepared and characterized by elemental analysis, spectroscopic and magnetic measurements. The proton-ligand ionization constants were determined potentiometrically using Irving–Rossotti technique. The stability constants of complexes were also calculated and were found in agreement with the seq

uence of stability constants of Irving and Williams. Thermal stability and degradation kinetics have been measured using thermogravimetric analyzer. Kinetic parameters were obtained for each stage of thermal degradation of complexes using Coats–Redfern method.


*Keywords:* Synthesis; Thermal degradation kinetics; Spectroscopic; Girard-P derivative

## 1. Introduction

Because of their capability to form water-soluble hydrazones, the girard-P 1-(carboxymethyl)pyridinium chloride hydrazide and the girard-T (carboxymethyl) trimethylammonium chloride hydrazide reagents, have long been used in organic chemistry to separate carbonyl compounds from other classes of organic substances [1,2]. Girard-P reagent has already been used to deprotect imino groups in cephalosporin chemistry [3]. Recently, a very efficient method of preparation of sultamicillin base was done by deprotection with girard-P reagents [4].

From a series of 33 thioacetals and hydrazones of 2-(4-formylstyryl)-5-nitro-1-vinylimidazole was prepared and examined for antitrypanosomal properties. The thioacetals were inactive as antitrypanosomal agents but three hydrazones derived from N-aminoguanidine, pyridylacethohydrazide chloride (girard reagent P), and dimethylaminoacetohydrazide (girard reagent D) displayed good activity against Trypanosoma rhodesiense [5].

Finally, in view of the fact that these reagents and their Schiff bases posses ligating atoms they have also been studied as ligands in coordination chemistry [6–8].

The present paper deals with the syntheses, spectral and thermal degradation kinetics of new series of transition metal complexes of 1-acetylpyridinium chloride-4-benzoyl thiosemicarbazide ($H_2$GPBzIT). Ligand formation constants and stability constants of all studied complexes were determined in solution potentiometrically using Irving–Rossotti technique. The thermal degradation kinetic parameters such as energy of activation ($E_a$) and the pre-exponential factor ($A$); and thermodynamic parameters like entropy ($\Delta S$), enthalpy ($\Delta H$) and activation energy ($\Delta G$) for each step of degradation have been evaluated.

## 2. Experimental

### 2.1. Instrumentation and materials

All starting materials were purchased from Fluka, Riedel and Merk and used without further purification. Elemental analyses (C, H, N) were performed on a Perkin-Elmer 2400 Series II Analyzer. Electronic spectra were recorded on a UV-UNICAM 2001 spectrophotometer using 10 mm pass length quartz cells at room temperature. Magnetic susceptibility was measured with a Sherwood Scientific magnetic susceptibility balance at 297 K. Infrared spectra were recorded on a Perkin-Elmer FT-IR Spectrometer 2000 as KBr pellets and as Nujol mulls in the 4000–370 $cm^{-1}$ spectral range. $^1$H NMR measurements at room

* Corresponding author. Tel.: +966 553901011.
*E-mail addresses:* usama@mans.edu.eg, uelayaan@kfu.edu.sa (U. El-Ayaan).

1386-1425/$ – see front matter © 2006 Elsevier B.V. All rights reserved.
doi:10.1016/j.saa.2006.11.016

Table 1
Analytical and physical data of $H_2$GPBzIT ligand and its metal complexes

| Compound | F. Wt. | Color | Found (Calculated) (%) | | | | | |
|---|---|---|---|---|---|---|---|---|
| | | | C | H | N | S | M | Cl |
| $H_2$GPBzIT $C_{15}H_{15}Cl\,N_4O_2S$ | 350.82 | White | 51.10 (51.35) | 4.25 (4.31) | 15.85 (15.97) | 9.19 (9.14) | – | – |
| $[Mn(HGPBzIT)_2(H_2O)_2]$ $C_{30}H_{32}Cl_2MnN_8O_6S_2$ | 790.60 | Pale yellow | 45.31 (45.58) | 3.96 (4.08) | 14.05 (14.17) | 8.21 (8.11) | 6.81 (6.95) | 9.02 (8.97) |
| $[Cr(HGPBzIT)Cl_2(H_2O)]$ $C_{15}H_{16}Cl_3CrN_4O_3S$ | 490.73 | Green | 37.3 (36.71) | 3.70 (3.29) | 11.20 (11.42) | 6.88 (6.53) | 10.62 (10.59) | 21.54 (21.67) |
| $[Co(HGPBzIT)Cl]$ $C_{15}H_{14}Cl_2CoN_4O_2S$ | 444.2 | Blue | 40.86 (40.56) | 3.21 (3.18) | 12.80 (12.61) | 7.46 (7.22) | 13.02 (13.27) | 15.84 (15.96) |
| $[Zn(HGPBzIT)Cl](H_2O)_2$ $C_{15}H_{18}Cl_2N_4O_4SZn$ | 486.69 | Pale yellow | 37.22 (37.02) | 3.68 (3.73) | 11.30 (11.51) | 6.69 (6.54) | 13.51 (13.43) | 14.62 (14.57) |
| $[Ni(GPBzIT)(H_2O)]$ $C_{15}H_{15}ClN_4NiO_3S$ | 425.52 | Brown | 42.43 (42.34) | 3.66 (3.55) | 12.94 (13.17) | 7.35 (7.53) | 13.52 (13.79) | 8.14 (8.33) |
| $[Cu_2(GPBzIT)\,Cl_2(H_2O)_2]$ $C_{15}H_{17}Cl_3Cu_2N_4O_4S$ | 582.84 | Brown | 30.86 (30.91) | 2.68 (2.94) | 9.71 (9.61) | 5.63 (5.50) | 22.02 (21.80) | 18.32 (18.25) |
| $[Cd_2(GPBzIT)\,(OAc)_2(H_2O)_2]$ $C_{19}H_{23}ClCd_2N_4O_8S$ | 727.75 | Yellow | 30.78 (30.89) | 2.98 (3.19) | 7.89 (7.70) | 4.52 (4.41) | 30.62 (30.89) | 4.94 (4.87) |

temperature were obtained on a Jeol JNM LA 300 WB spectrometer at 400 MHz, using a 5 mm probe head in $CDCl_3$. Chemical shifts are given in ppm relative to internal TMS (tetramethylsilane). Thermogravimetric measurements were performed on a DTG-50 Shimazu instrument.

### 2.2. Synthesis of 1-acetylpyridinium chloride-4-benzoyl thiosemicarbazide ($H_2$GPBzIT)

Preparation of 1-acetylpyridinium chloride-4-benzoyl thiosemicarbazide ($H_2$GPBzIT) was carried out by refluxing 4.8 g of girard-P with 4 ml benzoyl isothiocyanate in 20 ml absolute ethanol over a water bath for 4 h. The reaction mixture was left to cool till white crystals were separated out. These were filtered off, recrystallized from ethanol and finally dried in vacuum desiccators over anhydrous calcium chloride.

Yield: 6.50 g (74%) of ($H_2$GPBzIT). Found: C, 51.10; H, 4.25; N, 15.85. Calc. for $C_{15}H_{15}ClN_4O_2S$ (350.82): C, 51.35; H, 4.31; N, 15.97%.

### 2.3. Synthesis of metal complexes

All complexes were prepared by refluxing $H_2$GPBzIT (0.35 g, 1.0 mmol) and the hydrated metal salts (1.0 mmol), e.g. chloride and acetate, in 30 ml ethanol for 2–3 h. The resulting solid complexes were filtered while hot, washed with ethanol followed by diethyl ether and dried in vacuo over $CaCl_2$.

## 3. Results and discussion

The analytical and physical data of ($H_2$GPBzIT) ligand and its complexes are listed in Table 1.

### 3.1. IR and NMR spectra of H2GPBzIT ligand and its complexes

The principle IR bands of $H_2$GPBzIT and its metal complexes are listed in Table 2.

IR spectra (KBr) of $H_2$GPBzIT, show a three bands at 3236, 3123 and 3078 $cm^{-1}$ assigned to $\nu$NH(4), $\nu$NH(1) and

Table 2
Infrared data ($cm^{-1}$) of $H_2$GPBzIT ligand and its metal complexes

| Compound | IR ($cm^{-1}$) | | | | | | | |
|---|---|---|---|---|---|---|---|---|
| | $\nu(CO)_h$ | $\nu(CO)_b$ | $\nu$CS | $\nu$NH(4) | $\nu$NH(1) | $\nu$NH(2) | $\nu$(C–O) | $\nu$(C=N) |
| $H_2$GPBzIT | 1708 | 1676 | 704 | 3236 | 3123 | 3078 | – | – |
| $[Mn(HGPBzIT)_2(H_2O)_2]$ | 1730 | – | 695 | – | 3148 | 3052 | 1261 | 1662 |
| $[Cr(HGPBzIT)\,Cl_2(H_2O)]$ | – | 1666 | 711 | 3131 | – | 3053 | 1217 | 1598 |
| $[Co(HGPBzIT)Cl]$ | – | 1659 | 693 | 3131 | – | 3052 | 1213 | 1577 |
| $[Zn(HGPBzIT)Cl](H_2O)_2$ | 1680 | – | 706 | – | 3084 | 3062 | 1213 | 1598 |
| $[Ni(GPBzIT)(H_2O)]$ | – | – | 712 | – | – | 3064 | 1193<br>1208 | 1632<br>1600 |
| $[Cu_2(GPBzIT)Cl_2(H_2O)_2]$ | – | – | 712 | – | – | 3052 | 1197<br>1222 | 1628<br>1599 |
| $[Cd_2(GPBzIT)(OAc)_2(H_2O)_2]$ | – | – | 713 | – | – | 3052 | 1193<br>1208 | 1655<br>1590 |

b: benzoyl moiety; h: hydrozide moiety.

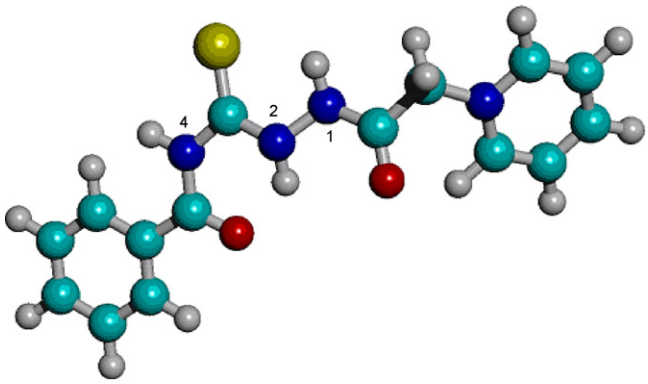


Fig. 1. Structure of the ligand ($H_2$GPBzIT).

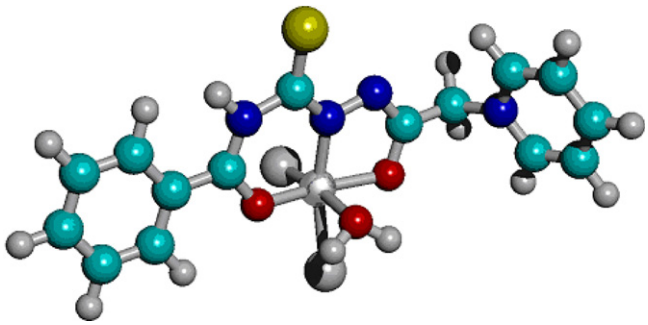

Fig. 2. Suggested structure of [Cr(HGPBzIT)$Cl_2(H_2O)$] complex.

$\nu$NH(2) modes, respectively. The two strong bands at 1708 and 1676 $cm^{-1}$ are attributed to $\nu$(CO) groups of the hydrazide(h) and benzoyl(b) moieties, respectively. Also, two bands at 704 and 1380 $cm^{-1}$ are assigned to $\nu$(CS) and a combination of ($\nu$CS + $\nu$CN) [9], respectively. The medium intensity band at 975 $cm^{-1}$ is attributed to the $\nu$(N–N) vibration [10]. No bands exist above 3500 $cm^{-1}$ or in the 2600–2500 $cm^{-1}$ [$\nu$(OH) and $\nu$(SH) vibrations] region. The absence of these bands indicates the presence of $H_2$GPBzIT in thione and keto form (Fig. 1). Weak bands at 1900–1800 $cm^{-1}$ are assigned to the stretching and bending vibrations (N–H–O). This result as well as the lowering of $\nu$NH suggests the presence of intramolecular hydrogen bonding [11].

The NMR spectrum of $H_2$GPBzIT in DMSO-$d_6$, shows three signals at $\delta$ = 9.28, 8.28 and 8.08 ppm relative to TMS which disappear upon adding $D_2O$ and can be assigned to NH(2), NH(4), NH(1) protons, respectively. The shift of $\delta$ NH to down field is due to hydrogen bonding. The multiplet at (7.35–9.1 ppm) are assigned to phenyl and pyridyl ring protons. The signal of $CH_2$ protons shifted to down field (6.36 ppm) because the presence of the quaternary nitrogen ($N^+$) which acts as a strong electron withdrawing group.

Infrared spectra of [Mn(HGPBzIT)$_2$($H_2O$)$_2$] complex show that the ligand behaves as a bidentate, coordinating *via* CS in the thione form and the enolized carbonyl oxygen of the benzoyl moiety with the displacement of a hydrogen atom from the latter group. This mode of coordination is supported by the following observations in the complex spectra: (i) the disappearance of both $\nu$(CO) of benzoyl moiety and $\nu$NH(4) with the simultaneous appearance of new bands assignable to $\nu$C–O and $\nu$(C=N); (ii) Bands assigned to $\nu$(CO) of hydrazide moiety are shifted to higher wavenumbers.

In the complexes, [Cr(HGPBzIT)$Cl_2(H_2O)$], [Co(HGPBzIT)Cl] and [Zn(HGPBzIT)Cl]$(H_2O)_2$, $H_2$GPBzIT behaves as a mononegative tridentate ligand. In the Cr(III) complex (Fig. 2) the ligand coordinating via the enolized carbonyl oxygen of the hydrazide moiety, the CO of the benzoyl moiety in the keto form and the nitrogen of NH group. In the Zn(II) complex, the ligand coordinates similarly but through the enolized carbonyl oxygen of benzoyl moiety. In Co(II) complex, the ligand coordinating via the enolized CO of hydrozide moiety, the CO of benzoyl moiety in the keto form and the CS in the thione form. The restricted rotation about the thiocarbonyl-nitrogen bond, the weak stability of seven membered ring and the lowering of $\mu_{eff}$ (4.26 BM) which may be due to antiferromagnetic interaction suggest the dimeric nature of Co(II) complex.

In the NMR of Zn(II) complex in DMSO-$D_6$, the signal assigned to NH(4) proton disappear as a result of $CO_b$ enolization. The absence of $H_2O$ signals indicate that $H_2O$ is out of coordination sphere.

In [Ni(GPBzIT)($H_2O$)], [$Cu_2$(GPBzIT)$Cl_2$($H_2O$)$_2$] and [$Cd_2$(GPBzIT)(OAc)$_2$($H_2O$)$_2$]$_2$ complexes, the ligand behaves as a binegative tridentate ligand through the enolic oxygen of both (CO) groups and the nitrogen of NH group. This behaviour is revealed by the disappearance of $\nu$(CO) for both benzoyl and hydrazide moieties, $\nu$NH(4) and $\nu$NH(1) with simultaneous appearance of new bands assignable to $\nu$(C–O) and $\nu$(C=N) groups. The dimeric nature of Cd(II) complex is confirmed from the NMR spectrum, where the signals integration of ligand protons corresponds a twice number of protons in the monomer of ligand. The sharpening of resonance and the shift of signal ($\delta$ 1.82 ppm) to higher field assigned to $CH_3$ protons of $CH_3COO^-$ as well as the absorption in the i.r. spectrum at 1560 $cm^{-1}$ demonstrates the formation of bidentate acetate [12,13]. All these observations suggested the structure of Cd(II) complex.

The color change of Cu(II) complex to green after addition of pyridine predicts the presence of chlorine bridge, which is further confirmed by the lowering of $\mu_{eff}$ (1.46 BM) which may be a result of strong antiferromagnetic interaction.

### 3.2. *Electronic spectra and magnetic moments*

Electronic spectra were measured in $10^{-3}$ M dimethyl sulfoxide (DMSO) solution of all studied complexes. The band positions, magnetic moments and calculated ligand field parameters are given in Table 3.

The electronic spectrum of [Cr(HGPBzIT)$Cl_2(H_2O)$] shows two strong absorption bands at 14,350 ($\nu_1$) and 21,650 $cm^{-1}$ ($\nu_2$). We could not observe the expected $\nu_3$ band on our instrument which might be hidden below $\nu_2$. The three spin-allowed transitions for chromium(III) in an octahedral field are as follows: $^4A_{2g}(F) \rightarrow {}^4T_{2g}(F)$ ($\nu_1$), $^4A_{2g}(F) \rightarrow {}^4T_{1g}(F)$ ($\nu_2$) and $^4A_{2g}(F) \rightarrow {}^4T_{1g}(P)$ ($\nu_3$). The $\nu_1$ transition is a direct measurement of the ligand field parameter 10 Dq. From $\nu_1$ and $\nu_2$, the value of $B$ and $\beta$ can be calculated. In addition, the $\mu_{eff}$-value

Table 3
Magnetic moment, electronic bands and ligand field parameters of the complexes derived from $H_2GPBzIT$

| Compound[a] | Band position ($cm^{-1}$) | Dq | $B$ | $\beta$ | $\mu_{eff}$ (BM) |
|---|---|---|---|---|---|
| $[Cr(HGPBzIT)Cl_2 \cdot H_2O]$ | 14,350, 21,650, 25,64, 27,933 | 1615 | 514.13 | 0.56 | 3.63 |
| $[Mn(HGPBzIT)_2(H_2O)_2]$ | 24,154, 26,954 | – | – | – | 6.70 |
| $[Ni(GPBzIT)(H_2O)]$ | 14,600, 20,964, 25,000 | – | – | – | 3.66 |
| [Co(HGPBzIT)Cl] | 14,662, 16,207, 19,080 | – | – | – | 4.26 |
| $[Cu_2(GPBzIT)Cl_2(H_2O)_2]$ | 12,610, 20,000, 25,900, 27,777 | – | – | – | 1.46 |

[a] Electronic spectra were measured in $10^{-3}$ M dimethyl sulphoxide (DMSO) solution of all studied complexes.

can be taken as additional evidence for the octahedral geometry [14].

The electronic spectrum of the $[Mn(HGPBzIT)_2(H_2O)_2]$ complex shows a strong band at 24,154 $cm^{-1}$ which is assigned to the $^6A_{1g} \rightarrow {}^4T_{2g}(D)$ transition. The other characteristic bands for d-d transitions are difficult to recognize in this complex and thus the ligand field parameters could not be calculated.

The electronic spectrum of $[Ni(GPBzIT)(H_2O)]$ is consistent with the tetrahedral geometry showing one broad d–d transition band at 14,600 $cm^{-1}$ assigned to $^3T_1(F) \rightarrow {}^3A_2(F)$ ($\nu_3$) transition. Magnetic moment of 3.66 BM is an additional evidence for the tetrahedral structure.

The electronic spectrum of the blue complex, [Co(HGPBzIT)Cl] exhibits an intense band at 14,662 $cm^{-1}$ assignable to the $^4A_2(F) \rightarrow {}^4T_1(P)$ transition and a shoulder at 16,207 $cm^{-1}$ due to spin coupling, indicating tetrahedral geometry for this complex. The blue color as well as the magnetic moment of 4.26 BM are a further indication for the tetrahedral geometry.

The lowering in $\mu_{eff}$ (1.46 BM) of the binuclear copper complex, $[Cu_2(GPBzIT)Cl_2(H_2O)_2]$ may be attributed to the covalent nature of the copper-sulphur bond. The electronic spectra show bands at 12,610, 20,000, 25,900 and 27,777 $cm^{-1}$ region. These band positions are in agreement with those generally observed for square-planar copper(II) complexes [15].

### 3.3. Potentiometric studies

#### 3.3.1. Determination of the proton-ligand Ionization constants

The ionization constants of 1-acetylpyridinium chloride-4-benzoyl thiosemicarbazide ($H_2GPBzIT$) was determined potentiometrically using Irving–Rossotti technique [16] at different temperatures (295, 308 and 318 K) and at constant ionic strength of 0.08 M KCl. At constant temperature of 295 K, the effect of different ionic strength on the proton-ligand ionization constant was studied using five different KCl concentrations. The ligand was titrated against carbonate-free sodium hydroxide (0.0105 M) solution. The titration curves for ($H_2GPBzIT$) and its metal complexes are shown in (Fig. 3) as a representative example.

The average number of protons associated with the ligand $\bar{n}_A$, was calculated at different pH-values using Irving–Rossotti equation [16]:

$$\bar{n}_A = Y - \frac{VN}{(V_0 - V)T_L}$$

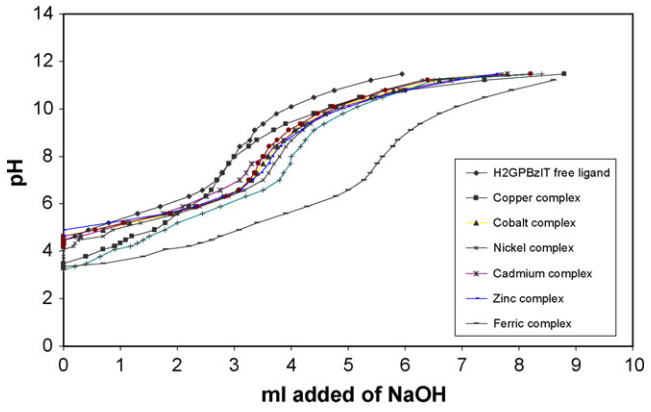


Fig. 3. Titration curves of metal ions–$H_2GPBzIT$ complexes, 0.2 M KCl at 295 K.

where $Y$ is the ionizable protons in the ligand, $V$ the volume of the alkali at desired pH, $V_0$ the initial volume of the titrated mixtures (25 ml in this study), $T_L$ the initial ligand concentration, and $N$ is the concentration of the alkali.

The proton-ligand formation curves are obtained by plotting $\bar{n}_A$ versus pH as shown in (Fig. 4). Same study was applied for other two temperatures namely, 308 and 318 K.

From these curves, the maximum $\bar{n}_A$ value was found to be ~1 indicating the presence of one dissociable amide proton in the ligand.

The proton-ligand stability constant ($pK_a$) of $H_2GPBzIT$ was determined by interpolation at half-$\bar{n}_A$ values, i.e. at $\bar{n}_A = 0.5$ from the $\bar{n}_A$-pH curves (Fig. 4). These values are confirmed by

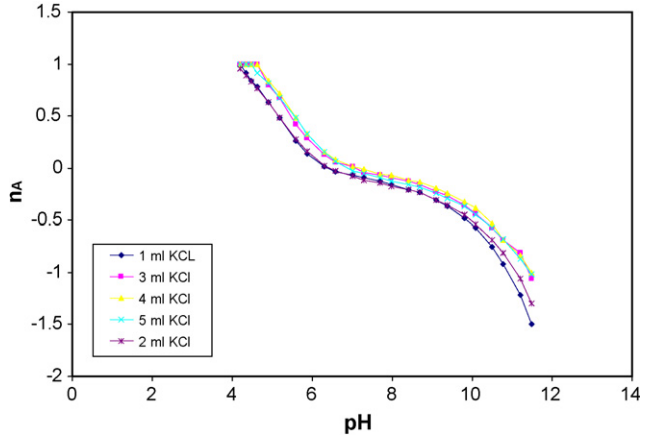


Fig. 4. Proton-ligand formation curves for $H_2GPBzIT$ using half-method at different ionic strength values.

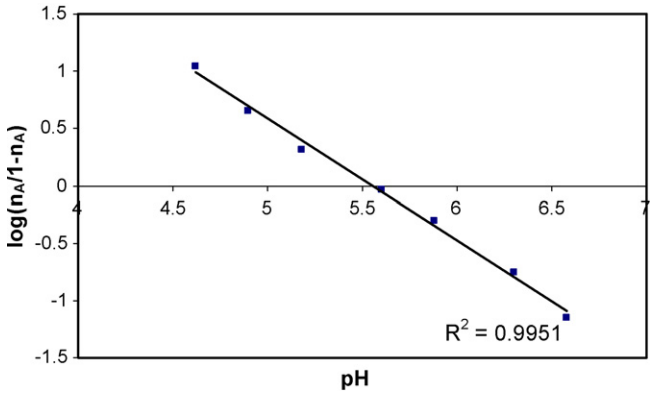


Fig. 5. Relation between $\log(\bar{n}_A/1-\bar{n}_A)$ vs. pH for proton-$H_2$GPBzIT, 0.20 M KCl and at 295 K.

the method of least square by plotting $\log(\bar{n}_A/1-\bar{n}_A)$ versus pH as shown in (Fig. 5).

The thermodynamic properties of solutions are not only useful for estimating the feasibility of reaction in solution, but they also offer one of the better methods for investigating the theoretical aspects of solution [17].

The standard free energy ($\Delta G^\circ$) associated with the acid dissociation can be calculated from the equilibrium constants of the reaction, as follow:

$$\Delta G^\circ = -2.303RT\,\mathrm{p}K_a$$

While the standard enthalpy change ($\Delta H^\circ$) of dissociation can be estimated from the use of Van't Hoff equation:

$$\frac{\mathrm{d}\ln K}{\mathrm{d}T} = \frac{\Delta H^\circ}{RT^2}$$

By plotting p$K_a$ versus $1/T$, from the slope the enthalpy change ($\Delta H^\circ$) for the dissociation of the ligand can be calculated.

Also, the standard entropy change ($\Delta S^\circ$) of dissociation can be calculated using the following well-known equation:

$$\Delta G^\circ = \Delta H^\circ - T\Delta S^\circ$$

The stoichiometric thermodynamic functions are summarized in Table 4. From these data the following conclusions can be obtained:

(a) p$K_a$ values decrease with increasing temperature, i.e. the acidity of the ligand increases with increasing temperature Table 4.

Table 4
Thermodynamic parameters and association constant for $H_2$GPBzIT (0.08 M KCl) at different temperatures

| Temperature (K) | p$K_a$ | $\Delta G^\circ$ (kJ mol$^{-1}$) | $-T\Delta S^\circ$ (kJ mol$^{-1}$) | $\Delta H^\circ$ (kJ mol$^{-1}$) |
|---|---|---|---|---|
| 295 | 5.60 | 31.63 | 4.68 | |
| 308 | 5.18 | 30.55 | 3.6 | 26.95 |
| 318 | 4.8 | 29.23 | 2.28 | |

Table 5
The association constants of $H_2$GPBzIT

| Method | p$K_a$ | | | | |
|---|---|---|---|---|---|
| | 0.04 M | 0.08 M | 0.12 M | 0.16 M | 0.20 M |
| Mid-point (half-method) | 5.2 | 5.3 | 5.5 | 5.6 | 5.6 |
| Least square method | 4.6 | 5.6 | – | 5.6 | 5.6 |

(b) The positive values of $\Delta H$ indicate that the dissociation processes are endothermic in nature and enhance with the rise of temperature.
(c) The negative values of $\Delta S$ are owing to the increasing of the order as a result of salvation process, which can be explained as the sum of the bound solvent molecules with the dissociated ligand being more than the solvent molecules originally accompanying the un-dissociated form.
(d) $\Delta G$ values for the dissociation constants are positive, i.e. the dissociation processes are non-spontaneous.
(e) The correlations of p$K_a$ values versus $1/T$ are linear in all cases, suggesting that $\Delta Cp$ values for the dissociation processes are zero over the studied temperature range (295–318 K).

We also studied the effect of differing the ionic strength on the proton-ligand stability constant and the result indicate that the values of p$K_a$ of the ligand decrease as the ionic strength increases due to inert salt effect (Table 5).

### 3.3.2. *Determination of stability constants of $H_2$GPBzIT complexes*

First-row transition metal complexes with $H_2$GPBzIT ligand have been studied potentiometrically. These include, Cu(II), Co(II), Ni(II), Zn(II), Fe(III) in addition to Cd(II). The titrations were performed at different ionic strength values ranging from 0.04 to 0.20 M KCl and at temperature of 295 K.

An inspection of the titration curves shown in (Fig. 3) for $H_2$GPBzIT reveals that the metal-ligand titration curves are below and well separated from the ligand titration curves. This indicates that the complexation processes were occurred with liberation of hydrogen ions.

The stability constant are evaluated from the formation curves drawn between $n$ and p$L$, where $n$ is the average number of ligand attached per metal ion and p$L$ is the free ligand exponent, $n$ values can be calculated from the following equation:

$$\bar{n} = \frac{T_L - [L]}{T_M}$$

where $T_L$ and $T_M$ are the initial concentrations of the ligands and the metal ion, respectively and $[L]$ is the ligand concentration at equilibrium. Therefore, the difference between $T_L$ and $[L]$ are the concentration of the bound ligand to the metal ion. The above equation can rewrite as follow:

$$n = \frac{(V2-V1)N^0}{(V_0+V_1)n_A T_M}$$

Table 6
The stability constants of metal ions–$H_2$GPBzIT complexes at different ionic strength of KCl and at 295 K

| Complex | p$K_a$ | | | | |
|---|---|---|---|---|---|
| | 0.04 M | 0.08 M | 0.12 M | 0.16 M | 0.20 M |
| $[Cu_2(GPBzIT)Cl_2(H_2O)_2]$ | 4.70 | 4.84 | 4.70 | 4.42 | 4.42 |
| [Co(HGPBzIT)Cl] | 3.3 | 3.3 | 2.60 | 2.60 | 2.60 |
| $[Ni(GPBzIT)(H_2O)]$ | 4.14 | 4.00 | 4.00 | 4.00 | 4.00 |
| $[Cd_2(GPBzIT)(OAc)_2(H_2O)_2]$ | 3.86 | 3.72 | – | – | – |
| $[Zn(HGPBzIT)Cl](H_2O)_2$ | 3.02 | – | 2.60 | 2.60 | 2.60 |
| [Fe–GPBzIT] | 4.84 | 4.84 | 4.84 | 4.84 | 4.84 |

where $V_2$ is the volume of alkali required to reach the desired pH in the mixture of complex solution and $T_M$ is the initial metal ion concentration.

The p$L$ value can be calculated by the following equation:

$$pL = \frac{\sum_{j=0}^{j=j} \beta_j H^j}{T_L - \bar{n}} \frac{V_2 + V_0}{V_0}$$

and for monobasic acid the following simplified form of equation can successfully apply [18]:

$$pL = pK_a - pH - \log\{[HA]_{init} - [OH^-]\}$$

The stoichiometric stability constants are evaluated using the half-method in which the following equation was applied:

$$\log K = \log\left(\frac{1}{[L]}\right)_{n=0.5}$$

(the p$K$ values are evaluated at $n = 0.5$)

The experimental stability constant values (Table 6) for complexation of the investigated ligands was found follows the order:

$$Co^{2+} < Ni^{2+} < Cu^{2+} > Zn^{2+}$$

In agreement with the will known sequence of stability constants of Irving and Williams [19], clearly this order reflects the changes in heats of complexation along the series and it arises from the influence of the polarization ability of the metal ions, as measured by the ratio of charge to ionic radius.

Moreover, Irving and Williams series is a consequence of crystal-field stabilization energy which varies in the order of $Co^{2+} < Ni^{2+} < Cu^{2+} > Zn^{2+}$, i.e. the splitting caused by the ligand in the energy level of the d-electrons diminishes the total energy of the system, thus causes in stabilization.

Also the results show that the trivalent metal ions are more stable than that of divalent ones, as a result of increasing the oxidation state.

### 3.4. Thermal analysis

Thermogravimetric (TG) and differential thermogravimetric (DTG) analysis were carried out for all studied complexes (Fig. 6).

In recent years there has been increasing interest in determining the rate-dependent parameters of solid state non-isothermal decomposition reactions by analysis of curves. Several equations [20–23] have been proposed as means of analyzing a TG curve and obtaining values for kinetic parameters. Many others [24–26] have discussed the advantages of this method over the conventional isothermal method. The rate of decomposition process can be described as the product of two separate functions of temperature and conversion [24], using:

$$\frac{d\alpha}{dt} = k(T) f(\alpha) \quad (1)$$

where $\alpha$ is the fraction decomposed at time $t$, $k(T)$ the temperature dependent function and $f(\alpha)$ is the conversion function dependent on the mechanism of decomposition. It has been established that the temperature dependent function $k(T)$ is of the Arrhenius type and can be considered as the rate constant $k$:

$$k = A\, e^{-E/RT} \quad (2)$$

where $R$ is the gas constant in (J mol$^{-1}$ K$^{-1}$). Substituting Eq. (2) into Eq. (1), we get:

$$\frac{d\alpha}{dt} = \left(\frac{A}{\varphi\, e^{-E/RT}}\right) f(\alpha) \quad (3)$$

where $\varphi$ is the linear heating rate d$T$/d$t$. On integration and approximation, this equation can be obtained in the following form:

$$\ln g(\alpha) = \frac{-E}{RT} \ln\left(\frac{AR}{\varphi E}\right) \quad (4)$$

where $g(\alpha)$ is a function of $\alpha$ dependent on the mechanism of the reaction. Several techniques have been used for the evaluation of temperature integral. In this work we use the integral method of Coats and Redfern to evaluate the kinetic parameters and study the thermal behavior of complexes using the following equations:

$$\ln\left[\frac{1-(1-\alpha)^{1-n}}{(1-n)T^2}\right] = -\frac{E}{RT} + \ln\left[\frac{AR}{\varphi E}\right] \quad \text{for } n \neq 1 \quad (5)$$

$$\ln\left[\frac{-\ln(1-\alpha)}{T^2}\right] = -\frac{E}{RT} + \ln\left[\frac{AR}{\varphi E}\right] \quad \text{for } n = 1 \quad (6)$$

where $A$ is the pre-exponential factor.

The correlation coefficient, $r$, was computed using the least square method for different values of $n$, by plotting the left-hand side of Eq. (5) or (6) versus 1000/$T$, Figs. 7 and 8. The $n$ value which gave the best fit ($r \cong 1$) was chosen as the order parameter for the decomposition stage of interest. From the intercept and linear slope of such stage, the $A$ and $E$ values were determined. The other kinetic parameters, $\Delta H$, $\Delta S$ and $\Delta G$ were computed using the relationships; $\Delta H = E - RT$, $\Delta S = R[\ln(Ah/kT)]$ and $\Delta G = \Delta H - T\Delta S$, where $k$ is the Boltzmann's constant and h is the Planck's constant. The kinetic parameters are listed in Table 7. The following remarks can be pointed out: (i) all complexes decomposition stages show a best fit for ($n = 1$) indicating a first order decomposition in all cases. Other $n$ values (e.g. 0, 0.33, and 0.66) did not lead to better correlations. (ii) The value of $\Delta G$ increases significantly for the subsequently decomposition stages of a given complex. This is due to increasing the

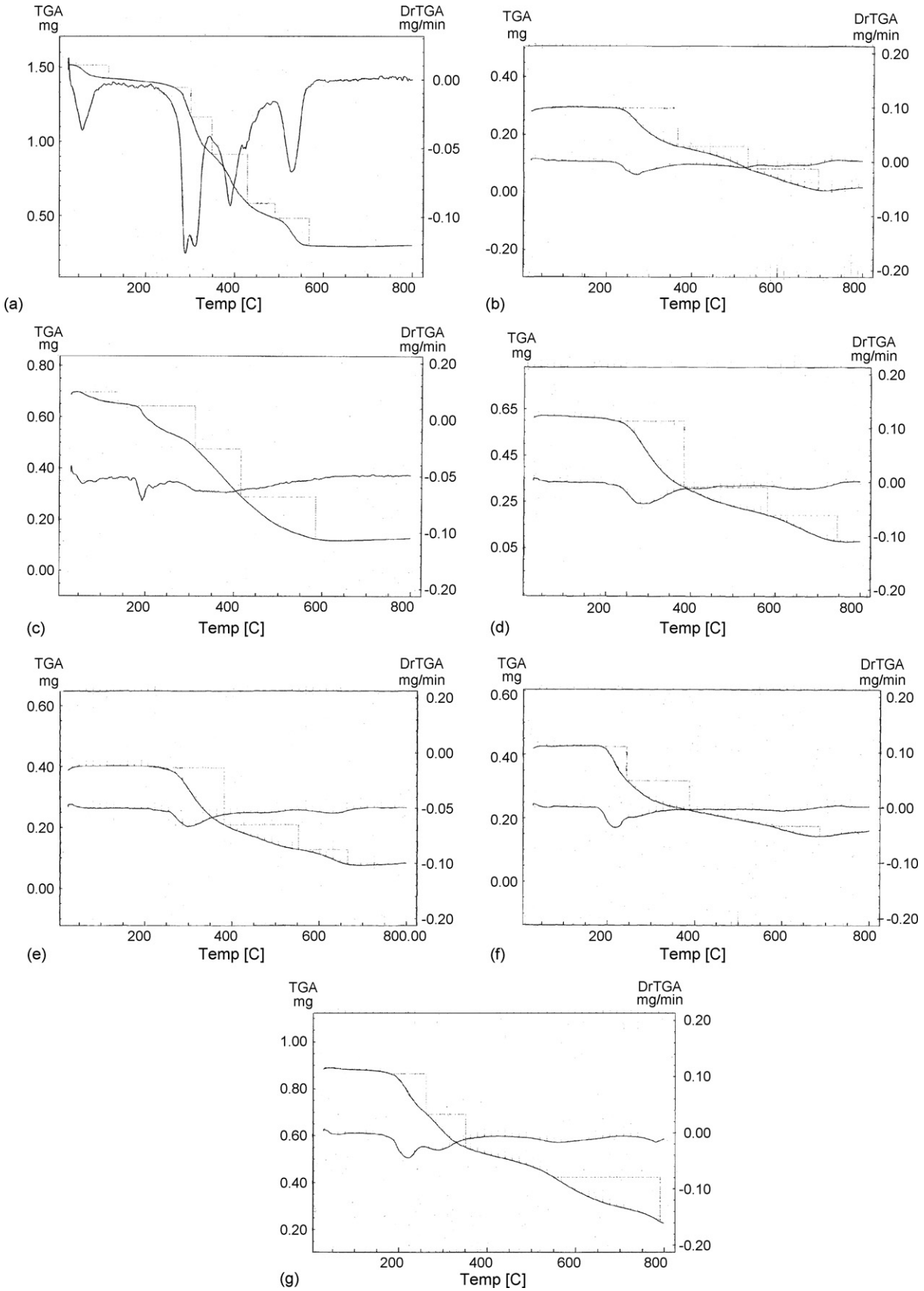


Fig. 6. TG and DTG of (a) [Ni(GPBzIT)($H_2O$)]; (b) [Mn(HGPBzIT)$_2$($H_2O$)$_2$]; (c) [Cr(HGPBzIT)$Cl_2$($H_2O$)]; (d) [Co(HGPBzIT)Cl]; (e) [Zn(HGPBzIT)Cl]($H_2O$)$_2$; (f) [$Cu_2$(GPBzIT)$Cl_2$($H_2O$)$_2$]; (g) [$Cd_2$(GPBzIT)(OAc)$_2$($H_2O$)$_2$] complexes.

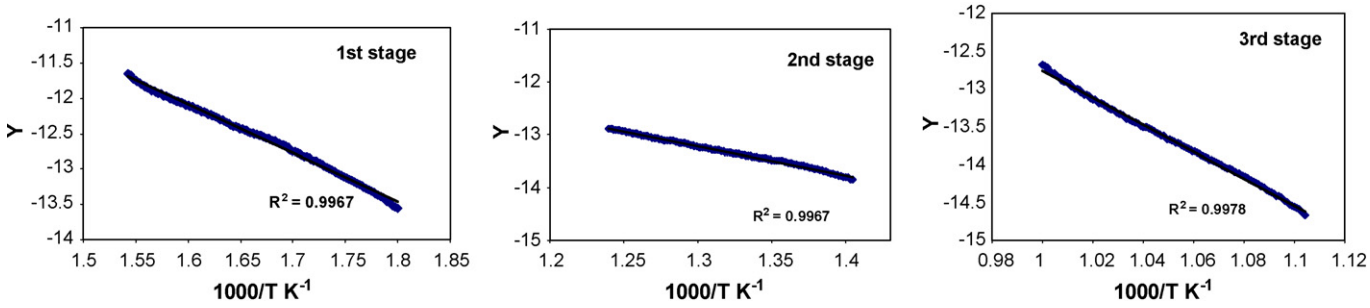


Fig. 7. Coats–Redfern plots of [Co(HGPBzIT)Cl] complex, where $Y = \ln[-\ln(1-\alpha)/T^2]$.

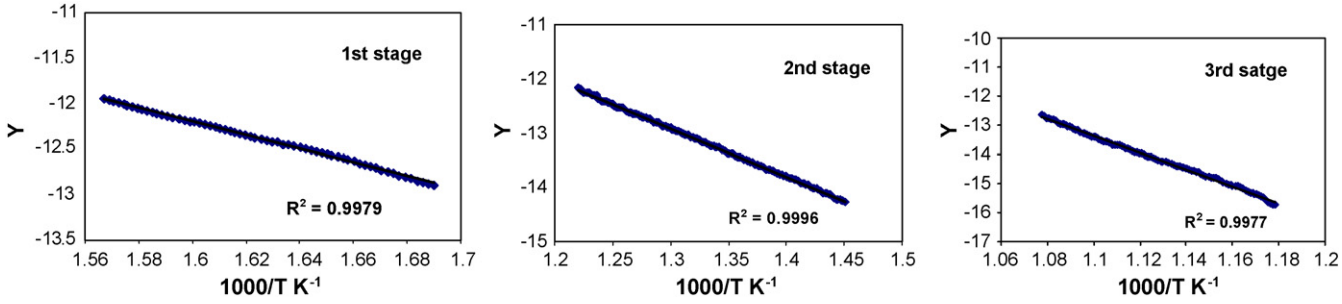


Fig. 8. Coats–Redfern plots of $[Zn(HGPBzIT)Cl](H_2O)_2$ complex, where $Y = \ln[-\ln(1-\alpha)/T^2]$.

values of $T\Delta S$ significantly from one stage to another which overrides the values of $\Delta H$. Increasing the values of $\Delta G$ of a given complex as going from one decomposition step subsequently to another reflects that the rate of removal of the subsequent ligand will be lower than that of the precedent ligand [27,28]. This may be attributed to the structural rigidity of the remaining complex after the expulsion of one and more ligands, as compared with the precedent complex, which require more energy, $T\Delta S$, for its rearrangement before undergoing any compositional change. (iii) The negative values of activation entropies $\Delta S$ indicate a more ordered activated complex than the reactants and/or the reactions are slow [29]. (iv) The positive values of $\Delta H$ mean that the decomposition processes are endothermic.

Table 7
Temperature of decomposition and the kinetic parameters of studied complexes

| Compound | Stage | $T$ (K) | $A$ ($S^{-1}$) | $E$ (kJ $mol^{-1}$) | $\Delta H$ (kJ $mol^{-1}$) | $\Delta S$ (kJ $mol^{-1}$ $K^{-1}$) | $\Delta G$ (kJ $mol^{-1}$) |
|---|---|---|---|---|---|---|---|
| [Ni(GPBzIT)($H_2O$)] | 1st | 336 | $6.38 \times 10^4$ | 45.1 | 42.4 | −0.154 | 94 |
| | 2nd | 590 | $2.90 \times 10^8$ | 121.1 | 116.2 | −0.088 | 168 |
| | 3rd | 662 | $5.3 \times 10^{10}$ | 165.5 | 160 | −0.046 | 190 |
| | 4th | 722 | $3.2 \times 10^9$ | 164.6 | 158.6 | −0.07 | 209 |
| [Mn(HGPBzIT)$_2$($H_2O$)$_2$] | 1st | 555 | 102.5 | 51.5 | 46.5 | −0.211 | 164 |
| | 2nd | 740 | 299.7 | 73.9 | 67.8 | −0.205 | 220 |
| | 3rd | 874 | $8.30 \times 10^5$ | 143.4 | 136.2 | −0.140 | 259 |
| [Cr(HGPBzIT)Cl$_2$($H_2O$)] | 1st | 353 | $8.1 \times 10^4$ | 15.0 | 12.0 | −0.152 | 66 |
| | 2nd | 500 | 0.189 | 20.8 | 16.6 | −0.263 | 148 |
| | 3rd | 636 | $2 \times 10^5$ | 95.2 | 89.9 | −0.150 | 185 |
| | 4th | 745 | 71.5 | 66 | 60 | −0.217 | 222 |
| [Co(HGPBzIT)Cl] | 1st | 573 | 369.5 | 57.0 | 52.2 | −0.20 | 168 |
| | 2nd | 726 | 2.14 | 45.7 | 39.7 | −0.246 | 219 |
| | 3rd | 930 | $4.6 \times 10^5$ | 148 | 140 | −0.146 | 276 |
| [Zn(HGPBzIT)Cl]($H_2O$)$_2$ | 1st | 585 | 960.6 | 62 | 57 | −0.193 | 170 |
| | 2nd | 723 | 397 | 74 | 68 | −0.203 | 214 |
| | 3rd | 887 | $3.8 \times 10^{11}$ | 239 | 232 | −0.032 | 261 |
| [$Cu_2$(GPBzIT)Cl$_2$($H_2O$)$_2$] | 1st | 560 | 0.60 | 25 | 20.3 | −0.254 | 163 |
| | 2nd | 880 | $3.2 \times 10^9$ | 202.9 | 195.6 | −0.072 | 259 |
| [$Cd_2$(GPBzIT)(OAc)$_2$($H_2O$)$_2$] | 1st | 495 | $7 \times 10^5$ | 77.2 | 73.1 | −0.137 | 141 |
| | 2nd | 624 | $4.5 \times 10^6$ | 98.9 | 93.8 | −0.124 | 171 |
| | 3rd | 913 | 36.5 | 78 | 70.4 | −0.238 | 288 |

## 4. Conclusion

In solution, the stability constant of complexes was found follows the order: $Co^{2+} < Ni^{2+} < Cu^{2+} > Zn^{2+}$, in agreement with the will known sequence of stability constants of Irving and Williams.

In solid state, the thermal decomposition kinetics of studied complexes reveals a first order decomposition in all cases. In addition, the kinetic parameters ($E$, $\Delta H$, $\Delta S$ and $\Delta G$) of all thermal decomposition stages have been calculated.

## References

[1] O.H. Wheeler, J. Chem. Educ. 45 (1968) 435.
[2] K. Toya, Nippon Naibunpi Gakkai Zasshi 64 (1988) 310.
[3] T. Watanabe, S. Sugawara, T. Miyadera, Chem. Pharm. Bull. 30 (1982) 2579.
[4] C. del Pozo, E. Alonso, F. Lopez-Ortiz, F. Fernandez-Mari, M. Bayod, J. Gonzalez, Tetrahedron 57 (2001) 6209.
[5] W.J. Ross, W.B. Jamieson, J. Med. Chem. 18 (1975) 158.
[6] A.A. El-Asmy, M.M. Mostafa, Polyhedron 2 (1983) 591.
[7] X. Wang, X.M. Zhang, H.X. Liu, Inorg. Chim. Acta 223 (1994) 193.
[8] X. Wang, X.M. Zhang, H.X. Liu, J. Coord. Chem. 33 (1994) 223.
[9] C.N.R. Rao, R. Venkataraghavan, Spectrochim. Acta 18 (1962) 541.
[10] D.N. Sathyanarayana, D. Nicholls, Spectrochim. Acta Part A 34 (1978) 263.
[11] J.I. Bullok, H.A. Tajmir-riahi, J. Chem. Soc. Dalton Trans. 34 (1978).
[12] S. Doeuff, M. Henry, C. Sanchez, J. Livage, J. Non-Cryst. Solids 89 (1987) 206.
[13] W. Wang, D. Jia, Y. Zhou, F. Ye, Mater. Res. Bull. 37 (2002) 2517.
[14] U. El-Ayaan, G. Abu El-Reash, I.M. Kenawy, Synth. React. Inorg. Met.: Org. Chem. 30 (2000) 1759.
[15] L. Sacconi, M. Ciampolini, J. Chem. Soc. (1964) 276.
[16] H.M. Irving, H.S. Rossotti, J. Chem. Soc. (1954) 2904.
[17] N.T. Abdel-Ghani, Y.M. Issa, M.A. Khaled, M.H. Kottany, Thermochim. Acta 125 (1988) 163.
[18] A. Albert, E.P. Serjeant, The Determination of Ionization Constants, Chapman and Hall Ltd., London, 1971.
[19] H.M. Irving, R.J.P. Williams, J. Chem. Soc. (1953) 3192.
[20] E.S. Freeman, B. Carroll, J. Phys. Chem. 62 (1958) 394.
[21] T. Ozawa, Bull. Chem. Soc. Jpn. 38 (1965) 1881.
[22] P. Kofstad, Nature 179 (1957) 1362.
[23] H.H. Horowitz, G. Metzger, Anal. Chem. 35 (1963) 1464.
[24] J. Šesták, V. Šatava, W.W. Wendlandt, Thermochim. Acta 7 (1973) 333.
[25] A.W. Coats, J.P. Redfern, Nature 201 (1964) 68.
[26] W.W. Wendlandt, Thermal Methods of Analysis, Wiley, New York, 1974.
[27] P.B. Maravalli, T.R. Goudar, Thermochim. Acta 325 (1999) 35.
[28] K.K.M. Yusuff, R. Sreekala, Thermochim. Acta 159 (1990) 357.
[29] A.A. Frost, R.G. Pearson, Kinetics and Mechanism, Wiley, New York, 1961.